Computational Materials Science 78 (2013) 34–38

Contents lists available at SciVerse ScienceDirect

Computational Materials Science

journal homepage: www.elsevier.com/locate/commatsci

Mechanism of the superior mechanical strength of nanometer-sized metal single crystals revealed

N.D. Afify [a], H.G. Salem [b], A. Yavari [c], T. El Sayed [d,*]

[a] Egypt Nanotechnology Research Center, El-Sheikh Zayed City, Giza, Egypt
[b] Department of Mechanical Engineering, The Yousef Jameel Science and Technology Research Center, The American University in Cairo, AUC Avenue, New Cairo 11835, Egypt
[c] School of Civil and Environmental Engineering, Georgia Institute of Technology, Atlanta, GA 30332, USA
[d] Computational Solid Mechanics Laboratory, Division of Physical Sciences and Engineering, King Abdullah University of Science and Technology, Thuwal 23955-6900, Saudi Arabia

ARTICLE INFO

Article history:
Received 18 January 2013
Received in revised form 4 May 2013
Accepted 14 May 2013

Keywords:
Nano-crystalline metals
Aluminum single crystals
Molecular dynamics simulation

ABSTRACT

Clear understanding of the superior mechanical strength of nanometer-sized metal single crystals is required to derive advanced mechanical components retaining such superiority. Although high quality studies have been reported on nano-crystalline metals, the superiority of small single crystals has neither been fundamentally explained nor quantified to this date. Here we present a molecular dynamics study of aluminum single crystals in the size range from 4.1 nm to 40.5 nm. We show that the ultimate mechanical strength deteriorates exponentially as the single crystal size increases. The small crystals superiority is explained by their ability to continuously form vacancies and to recover them.

1. Introduction

Nano-crystalline materials (conventionally with sizes below 100 nm) usually exhibit superior mechanical strength compared to their polycrystalline counterparts [1–5]. In recent years, this fact has attracted the attention of researchers who are seeking to fabricate advanced classes of bulk metals starting from these nanostructures. Furthermore, optimized consolidation and sintering methods have been developed in an attempt to allow for retention of the nanometer-scale properties in the bulk product [1,2]. Creating such bulk materials is not a simple task, however. To benefit from the superior nanometer-scale features in designing innovative mechanical components for specific applications, a clear understanding of the behavior of the starting nano-crystalline precursors is crucial.

The mechanical properties of nano-crystalline metals have been experimentally and computationally investigated either as single crystals [6,10–12,14–18] or polycrystalline [7–9,13]. Although of these high quality publications no clear quantification of the superiority of small single crystals and no clear explanation of such superiority were concluded. Consequently, no concrete conclusions on how to retain the nanometer-scale properties in the derived bulk materials could be obtained.

As the size of materials reduces down to the nanometer-scale, their experimental characterization becomes extremely difficult, if not impossible. On the contrary, using computational methods, such as molecular dynamics simulations, becomes convenient to understanding the atomic-scale origins of the peculiar mechanical properties of nano-crystalline materials as well as their dependencies on crystal size and different processing scenarios. The ability of molecular dynamics simulations to accurately capture the correct behavior of materials depends on many factors, among which are the availability of sufficient computational resources, the accuracy of interatomic potentials, adaptation of the correct simulation framework depending on the problem at hand, the level of analysis and visualization, and, of course, the critical interpretation of results.

In this article we present a molecular dynamics study of the dependence of the mechanical properties of nano-crystalline aluminum, in the single crystal form, on crystal size. The results reported in this article are part of a more detailed study aiming to fabricate bulk materials with advanced mechanical properties starting from aluminum nano-crystals. We believe that having a clear understanding of the mechanical behavior of single crystals will allow the possibility of the preservation of their superior properties when we deal with derived polycrystalline materials. In future communications, we will present an optimized sintering procedure for fabricating bulk materials that can better retain the advanced nanoscopic mechanical properties.

2. Computational methods

We study single aluminum crystals in the size range from 4.1 nm to 40.5 nm. The number of atoms in the studied samples

* Corresponding author. Tel.: +966 544700060.
E-mail address: tamer.elsayed@kaust.edu.sa (T. El Sayed).

0927-0256/$ - see front matter © 2013 Published by Elsevier B.V.
http://dx.doi.org/10.1016/j.commatsci.2013.05.011

ranged from 4000 to 4,000,000. In the following, we briefly describe our simulation framework. We use the Embedded Atom Method (EAM) [20,21]. The selected many-body potential was developed by Mishin et al. by fitting the potential againist both experimental and *ab-initio* datasets [19]. We selected this potential from other many-body potentials based on our evaluations of the predicted structures and mechanical properties of bulk aluminum. Molecular dynamics simulations were carried out using the Large-scale Atomic/Molecular Massively Parallel Simulator (LAMMPS) code [22]. The computational work was carried out on the IBM Blue Gene/P SHAHEEN supercomputer at King Abdullah University of Science and Technology (KAUST).

The starting atomistic configurations were prepared by stacking n = 10, 13, 16, 20, 30, 40, 50, 60, 70, 80, 90, and 100 ideal face-centered cubic (FCC) aluminum unit cells in three dimensions. The lattice constant for the employed interatomic potential was optimized to match the experimental value of 0.405 nm. The simulation time step was set to 0.001 ps. No periodic boundary conditions were assumed in any direction, since we are simulating samples of finite size, and are not interested in mimicking an infinite bulk material. Two 2.0 nm thick vacuum layers are placed at the top and bottom of the simulation box in the z-direction. The lowest and highest two atomic layers of atoms are kept fixed during the different simulation stages. Contrary to most published studies in this field, we do not apply any simple thermostatting schemes, such as the velocity scaling method or the Berendsen thermostat, since we are dealing with non-equilibrium molecular dynamics. Instead, we employ the so-called stochastic boundary conditions thermostatting scheme [23]. To achieve this, we couple the eight atomic layers adjacent to the fixed layers to the Langevin thermostat. The coupling between the simulated systems and the Langevin thermostat is weak enough such that no significant perturbations to the sample with smallest size is induced.

All simulations are conducted in the microcanonical ensemble (the atoms number, system volume, and energy are fixed). Molecular dynamics simulation of each sample comprised two main stages: (i) equilibration at 300 K for 500 ps, and (ii) continuous deformation at 300 K for 2000 ps. In the second stage, we carry out uniaxial tensile testing in the z-direction. The applied uniaxial strain ranged from 0.0 to 1.5 with an increment of 0.001. After each straining step, the system is left to evolve for 1.0 ps. This corresponds to a constant strain rate of $1.0 \times 10^9\ s^{-1}$. The calculated atomistic configurations are visualized using the AomEye package [24].

3. Results and discussion

Our molecular dynamics results are reported in Fig. 1. In Fig. 1a we report stress–strain curves of single aluminum crystals with sizes ranging from 4.1 nm to 40.5 nm. It should be noted that the stress and strain values reported here are the engineering ones. In qualitative agreement with the published literature [16,17], the stress–strain curve from a single crystal is typically formed by an elastic region where the stress increases quasi-linearly with the applied strain until it reaches a maximum, and then it decreases along the plastic deformation region. The first peak in our stress–strain curves is located at a strain value of ~0.1. The location of this peak slightly shifts to lower strain values with increasing the single crystal size. In Refs. [17,16], the locations of the main peaks were 0.035 and 0.2, respectively.

It should be noted that the quality of our stress–strain curves for nano-crystalline aluminum samples is excellent compared with the ones published in most of the relevant literature when periodic boundary conditions were not assumed. Thanks to the stochastic boundary conditions thermostatting scheme, there are no significant perturbations of the thermostat to the system's natural dynamics. Applying full periodic boundary conditions could also produce curves that are much less noisy due to the fact that energy conservation schemes are more accurate in this case, although this setting is not appropriate for simulating materials with finite sizes.

There are two major observations in Fig. 1a. First, the ultimate tensile strength of the material decreases as the crystal size increases. This result is highlighted in Fig. 1b (symbols) which shows the ultimate strength as a function of the crystal size. The strength values were calculated as the average of the highest ten data points on the first peak in the stress–strain curves. This curve can be fitted to an exponential decay function as shown by the red dotted line in Fig. 1b. From this figure, we can see that the material's strength depends strongly on the crystal size. In fact, the ultimate tensile strength decays exponentially as the crystal size increases. Such quantitative dependence of the ultimate tensile strength on the single crystal size has never been presented in literature in the case of metals.

The second major result, and probably the more interesting one in Fig. 1a is that the stress values, beyond the first stress peak, oscillate as a function of the applied strain with oscillation amplitudes dependent on the crystal size. In fact, small-sized nano-crystals have stress–strain curves with larger oscillations. As the crystal size increases, these oscillations decrease in amplitude and become smeared at 40.5 nm. In the following we explain the atomic-scale origins of these results through a detailed analysis of the calculated atomistic configurations.

We calculated the different coordination environments as a function of the applied strain and crystal size. Ideally, each aluminum atom should have 12 nearest neighbors in the first coordination shell. However, when the single crystal is strained, various coordination environments may occur simultaneously. In our atomistic configurations, we detected coordination numbers ranging from 5 to 13. Analysis of the different coordination environments as a function of crystal size and applied strain is a very important step in understanding the roles of different types of structural defects in determining a material's strength. Movies for each coordination environment as a function of the applied strain, and also a movie for the various coordination numbers represented by different colors, are available online as supplementary materials for the sample size of 20.2 nm.

The presence of 11-coordinated atoms indicates aluminum atoms that lack one nearest neighbor in the first coordination shell, and therefore represent atoms present near vacancies. Fig. 2a reports the concentration of vacancies as a function of the crystal size and applied strain. The vacancy concentration curves show one major peak located at a strain value of ~0.1 (i.e., coinciding with the first stress–strain peak). Furthermore, the location of this peak slightly shifts to lower strain values with increasing the crystal size, being consistent with the stress–strain curves. We observe that the concentration of vacancies decreases as the single crystal size increases. The most interesting result here is the observation that beyond the first stress–strain peak, the concentration of vacancies oscillates, with the peaks representing maximum population of vacancies and the dips representing recovery of vacant atoms. Furthermore, the amplitude of these oscillations decreases as the crystal size increases. We believe that the presence of such modulations in the density of vacancies is the major reason for the oscillations seen in the stress–strain curves. This correlation has never been demonstrated in the literature to this date.

To better understand this behavior of vacancies we report in Fig. 2b the concentration of dislocation cores, calculated as the concentration of the 13-coordinated aluminum atoms. From this figure it is clear that concentration of dislocation cores modulates as a function of the applied strain, in the same way the vacancies do. Furthermore, the amplitudes of these oscillations smear out

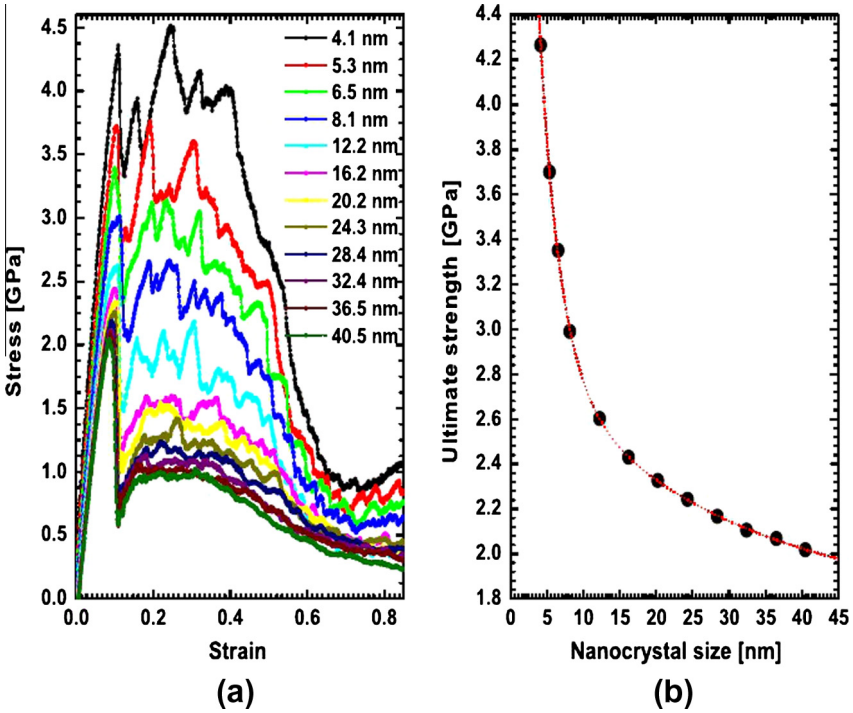

Fig. 1. Deformation behavior of single aluminum crystals in the size range from 4.1 nm to 40.5 nm: (a) stress–strain curves; and (b) ultimate strength as a function of crystal size. The strength values were fitted to an exponential decay function (shown by the red dotted line). (For interpretation of the references to color in this figure legend, the reader is referred to the web version of this article.)

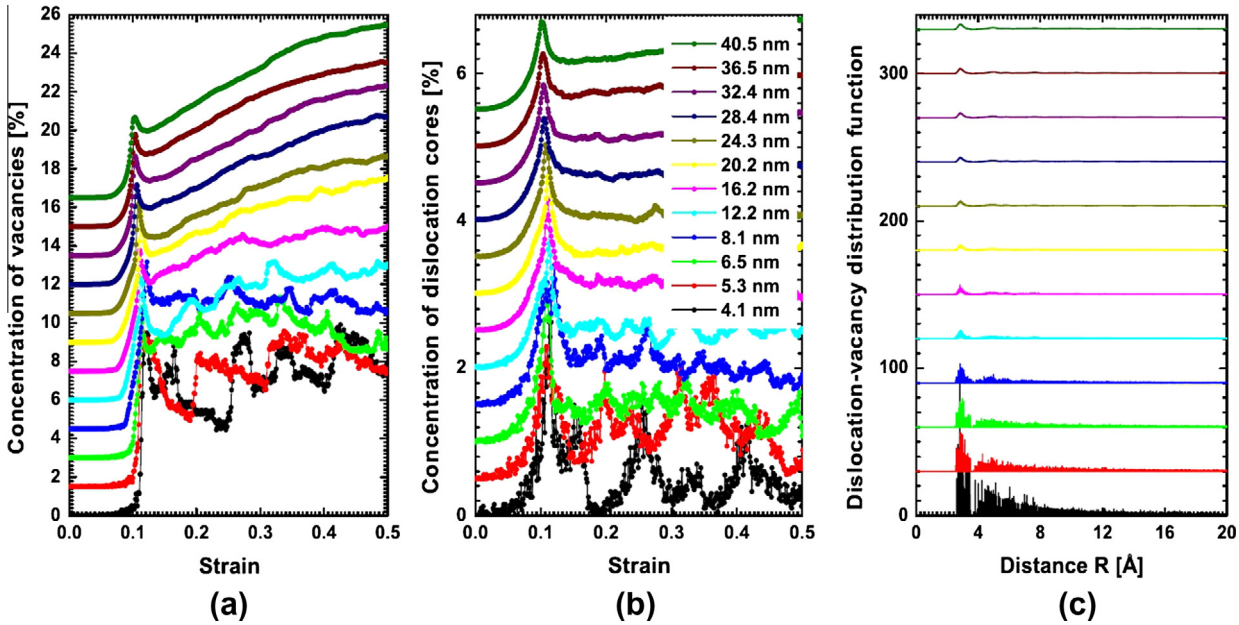

Fig. 2. Deformation behavior of single aluminum crystals in the size range from 4.1 nm to 40.5 nm: (a) concentration of vacancies, calculated as the concentration of the 11-coordinated aluminum atoms; (b) concentration of dislocation cores, calculated as the concentration of the 13-coordinated aluminum atoms; and (c) probability distribution function of vacancies around dislocation cores. Curves in the different figures are vertically shifted for clarity.

as the single crystal size increases. This is because in the small crystals vacancies are continuously forming and are annihilated by atoms from the nearby dislocations. From Fig. 2a and b we see that this kind of interaction becomes weak in the large crystals.

To confirm this result we report in Fig. 2c the probability distribution of vacancies around dislocation cores as a function of crystal size. The curves in this figure were normalized by the total number of dislocation–vacancy pairs persent in each sample. From this figure we see that for the sample with size of 4.1 nm there is a high probability of finding vacancies around dislocation cores. This probability decreases when the crystal size increases, and becomes almost independent of the crystal size beyond 10.0 nm. This explains the weak vacancy–dislocation interaction in the large single crystals. As we will demonstrate later, such large single crystals

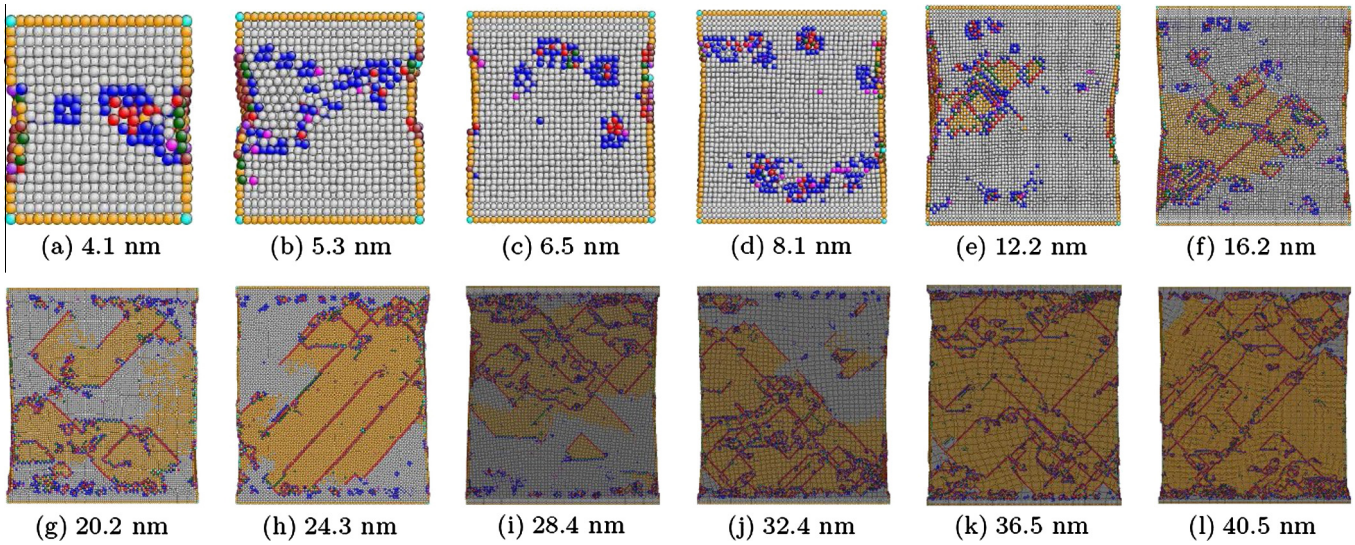

Fig. 3. The different coordination environments present in single aluminum crystals at a strain of 0.126 (i.e., at the first minimum after the main stress–strain peak) for different crystal sizes. Images were taken at distance of 0.5 nm from the actual crystal surface. The cyan, purple, brown, orange, green, red, blue, gray, and magenta colors represent the 5, 6, 7, 8, 9, 10, 11, 12, and 13-coordinated atoms, respectively. (For interpretation of the references to color in this figure legend, the reader is referred to the web version of this article.)

dissipate the applied stress through another mechanism, namely formation of grains at their surfaces. The oscillating behavior in vacancy concentration and the accompanying vacancy–dislocation interaction reported here clearly explains the jumps observed in the stress–strain curves of plastically deformed crystals [12], referred to therein as dislocation avalanches. Our results also explain the *in-situ* transmission electron microscopy tensile tests of aluminum single crystal [15], where it was argued that dislocations do escape from the crystal surfaces.

In Fig. 3, we show atomistic configurations of the samples with sizes of 4.1, 5.3, 6.5, 8.1, 12.2, 16.2, 20.2, 24.3, 28.4, 32.4, 36.5, and 40.5 nm. These snapshots were taken at a strain value of 0.126, i.e., at the first minimum after the main stress–strain peak. Atoms are colored according to their coordination environments. The 5, 6, 7, 8, 9, 10, 11, 12, and 13-coordinated atoms are represented by the cyan, purple, brown, orange, green, red, blue, gray, and magenta colors, respectively. The reported images were taken at distance of 0.5 nm from the actual crystal surface. In this figure, we see that the behavior of defects strongly depends on the size of the crystal. For crystals with large sizes such as from 12.2 to 40.5 nm, the formation of grains at the surfaces takes place already at a strain of 0.126. Furthermore, the formation of such grains takes place at the surface first, then evolves inside the material in the coarse of the tensile testing. Two movies comparing the formation of grains at distances of 0.5 and 1.0 nm from the surface of the largest simulated sample are available online as supplementary materials.

Let us consider the 8-coordinated atoms (represented by the orange color in Fig. 3). These atoms may represent free surfaces of grains or regions with disordered local structures. To track this situation as a function of crystal size, we calculated the density profile of the 8-coordinated atoms along the *x*-direction.These profiles are reported in the supplementary materials. For small crystals, we found that these aluminum atoms have a homogeneous distribution, which means that they are present in small regions of disordered local structures. On the contrary, for large crystals, the density profiles exhibit clear maxima, which indicates that a significant fraction of the 8-coordinated atoms represent free surfaces of grains. Furthermore, the fraction that represents free surfaces of grains increases as the size of single crystal increases. The tendency of large crystals to form grains at their surfaces can be explained by the small vacancy–dislocation interaction probability in this case, which leads to large growth of dislocations. This important result does not only confirm, but also visualizes the individual dislocation cells concept characterized by the spatially resolved X-ray measurements on a deformed copper single crystal [11].

4. Conclusions

In summary, we have presented a quantitative description of aluminum single crystals mechanical strength as a function of their size, and explained why small metal single crystals show higher strength. Aluminum single crystals mechanical strength decays exponentially as the crystal size increases. Small single crystals possess better strength due to their ability to continuously form vacancies and recover them. This study provides important findings that may allow for developing advanced bulk materials in which superior nano-scale mechanical properties can be retained.

References

[1] H. Salem, A. Sadek, AA 2124. J. Mater. Eng. Perform. 19 (2010) 356.
[2] H.G. Salem, S. El-Eskandarany, A. Kandil, H.A. Fattah, J. Nanomater. 2009 (2009) 479185.
[3] E. Bonetti, L. Pasquini, E. Sampaloesi, Nanostruct. Mater. 9 (1997) 611.
[4] X. Sun, H. Cong, M. Yang, M. Sun, Metall. Mater. Trans. A 31 (2000) 1017.
[5] A.S. Khan, Y.S. Suh, X. Chen, L. Takacs, H. Zhang, Int. J. Plast. 22 (2006) 195.
[6] V. Bulatov, F.F. Abraham, L. Kubin, B. Devincre, S. Yip, Nature 391 (1998) 669.
[7] V. Yamakov, D. Wolf, S.R. Phillpot, A.K. Mukherjee, H. Gleiter, Nature Mater. 1 (2002) 45.
[8] J. Schitz, K.W. Jacobsen, Science 301 (2003) 1357.
[9] Z. Shan, E. Stach, J. Wiezorek, J. Knapp, D. Follstaedt, S. Mao, Science 305 (2004) 654.
[10] E. Bringa, K. Rosolankova, R. Rudd, B. Remington, J. Wark, M. Duchaineau, D. Kalantar, J. Hawreliak, J. Belak, Nature Mater. 5 (2006) 805.
[11] L.E. Levine, B.C. Larson, W. Yang, M.E. Kassner, J.Z. Tischler, M.A. Delos-Reyes, R.J. Fields, W. Liu, Nature Mater. 5 (2006) 619.
[12] F.F. Csikor, C. Motz, D. Weygand, M. Zaiser, S. Zapperi, Science 318 (2007) 251.
[13] J. Rajagopalan, J.H. Han, M.T.A. Saif, Science 315 (2007) 1831.
[14] Z. Shan, R.K. Mishra, S.S. Asif, O.L. Warren, A.M. Minor, Nature Mater. 7 (2007) 115.
[15] S.H. Oh, M. Legros, D. Kiener, G. Dehm, Nature Mater. 8 (2009) 95.
[16] R. Komanduri, N. Chandrasekaran, L. Raff, Int. J. Mech. Sci. 43 (2001) 2237.
[17] L. Yuan, D. Shan, B. Guo, J. Mater. Process. Technol. 184 (2007) 1.

[18] X. Li, Y. Wei, W. Yang, H. Gao, Proc. Natl. Acad. Sci. USA 106 (2009) 16108.
[19] Y. Mishin, D. Farkas, M. Mehl, D. Papaconstantopoulos, Phys. Rev. B59 (1999) 3393.
[20] M.S. Daw, M.I. Baskes, Phys. Rev. B29 (1984) 6443.
[21] M.W. Finnis, J.E. Sinclair, Philos. Mag. A50 (1984) 45.
[22] S. Plimpton, J. Comp. Phys. 117 (1995) 1.
[23] D. Toton, C. Lorenz, N. Rompotis, N. Martsinovich, L. Kantorovich, J. Phys.: Condens. Matter. 22 (2010) 074205.
[24] J. Li, Modelling Simul. Mater. Sci. Eng. 11 (2003) 173.